UNIVERSITY OF AMSTERDAM

UvA-DARE (Digital Academic Repository)

ORIGINAL RESEARCH ARTICLE

Vadose Zone Journal OPEN ACCESS

Colloidal catchment response to snowmelt and precipitation events differs in a forested headwater catchment

Dymphie J. Burger[1,2] | **Johnny Vogel**[2,3] | **Annemieke M. Kooijman**[3] |
Roland Bol[2] | **Eva de Rijke**[3] | **Jorien Schoorl**[3] | **Andreas Lücke**[2] |
Nina Gottselig[1]

[1] Institute of Crop Science and Resource Conservation, Soil Science and Soil Ecology, Univ. of Bonn, Nussallee 13, Bonn 53115, Germany

[2] Forschungszentrum Jülich, Institute of Bio- and Geosciences, IBG-3: Agrosphere, Wilhelm Johnen Str, Jülich 52425, Germany

[3] Institute for Biodiversity and Ecosystem Dynamics, Univ. of Amsterdam, Science Park 904 GE, Amsterdam 1090, The Netherlands

Correspondence
Dymphie J. Burger, Institute of Crop Science and Resource Conservation, Soil Science and Soil Ecology, Univ. of Bonn, Nussallee 13, Bonn, Germany, 53115.
Email: dburger@uni-bonn.de

Assigned to Associate Editor Kenton Rod.

Abstract

Climate change affects the occurrence of high-discharge (HD) events and associated nutrient exports in catchment stream water. Information on colloidal events-based losses of important nutrients, such as organic C(C_{org}), N, P, and S, remain relatively scarce. We hypothesized that contributions of colloidal exported N, S, and P due to differing hydrological mechanisms vary between HD events in late winter and spring. We examined one combined snowmelt and rainfall event (March 2018) with one rainfall event (May 2018) for temporal C_{org}, N, P, and S dynamics. The catchment exports of colloids and their subset nanoparticles were analyzed by asymmetric-flow field flow fractionation (P) and a filtration cascade (N and S). The C_{org} source in both events was assessed by $\delta^{13}C$ composition of the stream water in relation to that of the soil. In winter, <6% of stream water P was transported by colloids (>0.1 μm), but this was 29–64% in spring and was associated with C_{org}, Fe, and Al. Colloidal N and particulate S (>1 μm) were higher during both events, but the majority of losses were dissolved (<0.1 μm). The $\delta^{13}C$ values of dissolved organic matter ($^{13}C_{DOM}$) showed that in winter, most C_{org} was exported from the hydrologically connected hillslopes by water flowing through mineral horizons, due to snowmelt. During and after the rainfall events, export from organic horizons dominated the nutrient losses as particulates, including colloids. These events highlight the need for a better quantification of often underreported particulate, colloid, and nanoparticle contributions to weather-driven nutrient losses from catchments.

1 | INTRODUCTION

Globally, weather driven transport in streams is one of the most important pathways of organic carbon (C_{org}), nitrogen (N), phosphorus (P), and sulfur (S) losses from catchments (Cole et al., 2007; Haygarth et al., 1998; Stacy et al., 2015). Due to climate change, mountainous areas in Germany are predicted to experience more precipitation events of

longer duration in winter and less frequent, but more intense, precipitation events during the summer (Federal German Government, 2015). Both winter and summer events are therefore predicted to create substantial peak discharges in streams and rivers, so-called "high-discharge (HD) events" (Gao et al., 2014), which may have detrimental effects on the ecology and water quality in the affected area (Kleinman et al., 2006; Park et al., 2010). Such HD events export nutrients from the soil and cause both a loss of nutrients upstream and increases downstream in the catchments (Yusop et al., 2006). Within the context of abovementioned climate change predictions, we need to further increase our understanding of the influence of such HD events on their associated substantial nutrient export from catchments (Inamdar et al., 2006).

Nitrate (NO_3^-), phosphate (PO_4^{3-}), and sulfate (SO_4^{2-}), the most readily available chemical forms of N, P, and S for plants, have different mobilities in soil systems. Although NO_3^- is mostly present in the soil solution and is mobile (Inamdar et al., 2006; McNeill et al., 2005), SO_4^{2-} can either be adsorbed to particles in the soil or is present in the soil solution, being mobile in the latter form (McNeill et al., 2005). Phosphate is mostly adsorbed to particles in the soil, since it is the preferred anion for adsorption over SO_4^{2-} and NO_3^- (Johnson & Cole, 1980). Therefore, P is often regarded as relatively immobile in solution, as it quickly precipitates, but whenever soil particles move due to erosion, P can be transported in a particulate form (Inamdar et al., 2006; McNeill et al., 2005; Sharma et al., 2017).

Organic forms of macronutrients and NH_4^+ show different behavior during export than NO_3^-, PO_4^{3-}, and SO_4^{2-} and should therefore be considered as well when examining the overall fate and export of N, P, and S species. Generally, in oxygen-rich water, NH_4^+ is transferred rapidly to NO_3^-. However, during HD events, nitrification is disrupted and NH_4^+ may be lost from the ecosystem by being exported further downstream (Johnson & Cole, 1980). Organic N, P, and S mainly stem from soil horizons rich in organic material, present there in larger quantities than their inorganic counterparts. However, organic N, P, and S are generally less mobile and therefore less abundant in stream water during baseflow. During overland flow events and after high-intensity rainfall events, however, these organic forms can be transported to the stream environment and lost from the catchment (Haygarth et al., 1998; Inamdar et al., 2011; Julich et al., 2017; Raymond & Saiers, 2010; Stutter et al., 2008; Tunaley et al., 2016).

Both catchment response and the availability of the different forms of N, S, P, and C_{org} differ per season (Penna et al., 2015; Strohmeier et al., 2013). In the wet winter season, precipitation can be in the form of snow, and precipitation is often of longer duration and lower intensity. In the drier late spring and summer season, precipitation is usually characterized by shorter and more intense precipitation events, snow being absent (Penna et al., 2015). This, in combination with

Core Ideas

- Overland flow contribution is critical in the spring event, in winter more by groundwater.
- P, N_{org}, and S_{org} coupled to C_{org} transport are most prominent for the spring event.
- Dissolved N and S dominate export losses, whereas particulates are more important in spring.
- Colloidal P dominates export loss, whereas in spring it is bound to C_{org}.
- Colloidal export N, S, and P spring losses are still often overlooked in export budgets.

seasonal differences in catchment wetness, can cause overland flow and export compounds from soil horizons richer in organic material (Penna et al., 2015). Low temperatures are known to inhibit microbial activity and plant growth, which causes high inorganic N, S, and P and low organic N, S, P, and C_{org} concentrations, increasing the availability the inorganic forms of N, S, and P for export in winter (Brooks et al., 1998; Fabre et al., 1996; Mitchell et al., 1992; Strohmeier et al., 2013).

As stated before, not all macronutrient species are exported in the dissolved state, and P and organic S (S_{org}) can both bind to C_{org} particles (Darch et al., 2014; Regelink et al., 2013; Scherer, 2009) and be transported by surface water as well as groundwater (Onstad et al., 2000). Furthermore, the source of C_{org} involved in the export may differ, which can be studied through its $\delta^{13}C$ value (Lambert et al., 2011; Onstad et al., 2000). They found that C_{org} depleted in $\delta^{13}C$ (around −30‰) originates from organic soil layers and C_{org} enriched in $\delta^{13}C$ (around −25‰) from mineral soil layers. Analysis of the source of C_{org} can help explain the active hydrological mechanisms in a catchment and the (seasonal) variation (Sebestyen et al., 2008).

Past studies have also shown that P export is often associated with the transportation of fine particles and colloids (Heathwaite et al., 2005; Sharpley et al., 2013; Stutter et al., 2008). Particularly natural colloids (1–1,000 nm; NC), as well as their subset natural nanoparticles (1–100 nm; NNP), are increasingly recognized as relevant carriers of nutrients in ecosystems due to their high specific surface area (Lead & Wilkinson, 2006). Phosphorus adsorbs to colloids consisting of primary building blocks such as C_{org}, Fe oxides, Al oxides, clays, and calcium carbonates (Crews et al., 1995; Domagalski & Johnson, 2011; Gottselig, Amelung et al., 2017; Gottselig, Nischwitz et al., 2017; Reddy et al., 1995; Sharpley et al., 2013). Especially small NC such as NNPs can be mobile and form substantial components in the context of associated element transport (Martin et al., 1995; Mayer & Jarrell, 1995; Philippe & Schaumann, 2014; Trostle et al., 2016).

Gottselig et al. (2014) studied general export dynamics of NNP and colloidal-bound Fe, Al, and P from different parts of the Wüstebach catchment and found that particle size and composition is controlled by tributary inflow, which is attributed to hydrological mechanisms and has consequences for their mobility. However, as this study was conducted during baseflow conditions, colloidal P transport during high-precipitation events was not considered in there. Colloidal export of N and S may be lower than for P, but data are scarce in any case. Rostad et al. (1997) showed that 1–3% of N was bound to colloids in the Mississippi River. Sulfate is often the only chemical species of S analyzed—for example, its occurrence after storm events (Mitchell et al., 2006) and specifications such as S_{org} are neglected. In Neubauer et al. (2013), S ($<0.2\,\mu m$) was mostly transported as sulfate during storm flow events in a catchment in the German Fichtelgebirge mountains, but in a single September event, a significant proportion was associated with colloids (Neubauer et al., 2013).

There is thus a need to resolve the role of NC for P export during high-precipitation events, but also its role for N and S binding and transport. However, a detailed assessment of the relevant colloidal bound chemical species (especially P) in forest ecosystems (Bol et al., 2016) is still lacking, especially during peak flow scenarios. Even many hypotheses on dissolved and overall P fluxes in natural ecosystems remain quantitatively untested (Bol et al., 2016; Lang et al., 2016).

The TERENO Wüstebach catchment is a well-studied, intensively monitored catchment in Germany (see Bogena et al., 2015, for details). Stockinger et al. (2014) found that the catchment riparian zone response differs from the hillslopes, and when the soil moisture content is below 35% (May until November), only the riparian zone is hydrologically active. However, even during this relatively dry season, the whole catchment may be active through preferential flow in response to high rainfall events (Wiekenkamp et al., 2016). Within the catchment, the source of the water of the different tributaries can be linked to the dissolved organic matter (DOM) and NO_3^- export (Weigand et al., 2017). Specifically, higher stream water C_{org} content implies that overland flow or subsurface flow through C_{org}–rich soil layers occurs, whereas high NO_3^- concentrations point to a groundwater-based origin (Bol et al., 2015; Weigand et al., 2017).

Based on the above, we formulated three hypotheses to describe the Wüstebach catchment during two events:

1. Dominating N, S, and P species and form (colloidal or dissolved) differ among events, which is (partly) coupled to increased organic C export. During HD events, P will be mainly exported in colloids, but N and S will be mainly in dissolved form.
2. Dominating N, S, and P species differ between late winter and spring events, due to different transport mechanisms

with more influence from groundwater in late winter and more overland flow and subsurface flow in spring.
3. Within the colloidal fractions, NNP are more mobile during events than larger colloids.

2 | MATERIALS AND METHODS

2.1 | TERENO test site Wüstebach

This study was carried out in the Wüstebach catchment, a small subcatchment of the river Rur, in the south of the Eifel/Lower Rhine Valley observatory of the Germany-wide climate change research network TERENO (Terrestrial Environmental Observatories). The Wüstebach catchment is located close to the Belgian border in the Eifel National Park, covers 38.5 ha, and varies in altitude from 595 to 628 m asl (Bogena et al., 2015; Graf et al., 2014; Stockinger et al., 2014). The average yearly precipitation of the Wüstebach catchment is 1,220 mm (1979–1999) (Bogena et al., 2010) and the average temperature is 7 °C (Zacharias et al., 2011).

The current vegetation is dominated by Norway spruce [*Picea abies* (L.) Karst] and Sitka spruce [*Picea sitchensis* (Bong.) Carrière], which were planted after 1945 (Etmann, 2009). In 2013, the spruce trees in the riparian zone were cut to create space to regenerate the endemic beech forest. The soils are formed on Devonian shale bed rock in a silty clay loam parent material with a large fraction of coarser material, in the category of 0.2 cm to several centimeters (Graf et al., 2014; Rosenbaum et al., 2012). The soils on the steeper hill slopes are mainly shallow, Cambisols and Planosols (Inceptisols in the USDA classification). Histosols and Gleysols (Histosols and Inceptisols in the USDA classification) are mostly found in the riparian zone (Bogena et al., 2015). At the outlet of the research catchment, the discharge is measured every 10 min by a V-notch weir for low flow periods and a Parshall flume to measure normal to high flows. TriOS-multi probes (YSI 6820; see Bogena et al., 2015), which measure the electrical conductivity, pH, and water temperature at the same location. Air temperature measurements come from a 38-m-high tower in the northwest of the catchment, precipitation is measured with and a heated standard Hellmann type tipping bucket rain gauge (Ecotech; see Bogena et al., 2018), located at the catchment's southern end. Both parameters are measured at a 10-min time interval (Bogena et al., 2015).

2.2 | Event sampling

In 2018, sampling was conducted during one high precipitation event in winter and one in spring. Characteristics of the events are given in Supplemental Table S1 and precipitation, temperature, and discharge are shown in Supplemental

Figure S1. The winter combined snowmelt and rainfall event was analyzed from 5 and 12 March 2018. In the first few days, small diurnal discharge peaks without rainfall were caused by snowmelt as temperatures were above zero during the afternoon. Precipitation fell on 8 and 9 March, leading to a coupled snowmelt and rainfall event. Prior to the March event, climatic conditions were dry as last non-snow precipitation occurred on the 12 February, but due to a 30-cm snow cover, the antecedent catchment wetness was high. Furthermore, temperatures were below zero with a minimum of −14.6 ˚C in the 3 wk prior to the event. The rise in temperature and the following rainfall created a long-lasting catchment response stretching over several days. The spring event, consisting of a high-intensity rainfall event, sparking a quick and short catchment discharge response on 16 and 17 May 2018. Two other rain showers occurred 6 and 2 d prior to the event, in the week before these two minor events one dry week with high temperatures (maximum temperatures up to 23 ˚C) was recorded. In March, the soil moisture of the catchment is usually high, meaning that hydrological connectivity between riparian zone and hillslope soils was present and the catchment was mainly saturated. In May, the soil moisture is on average lower, meaning that probably only the riparian zone was hydrologically active (Rosenbaum et al., 2012; Stockinger et al., 2014).

An automatic sampler (ASW Ecotech) installed at the outlet of the catchment was programmed to sample stream water in 24 600-ml polyethylene bottles at set time intervals, starting at a predefined threshold water level. This threshold was set as close as possible to current base flow conditions without reacting to non-event-related water table changes. This allowed a sampling of the majority of the rising limb of the hydrograph. The sampling time intervals were adjusted to the expected duration of the event, longer in winter due to co-occurrence with snowmelt and short in summer due to higher precipitation intensity expected. This was every 8 h in winter, increasing the sampling frequency to 50 min after an increasing water level and every half an hour in spring, as a short-term event was expected.

2.3 | Sample treatment and chemical analysis

The autosampler samples of the March 2018 (winter) and May 2018 (spring) event were both filtered at 0.45 μm (PES filter; GE Healthcare) or left untreated. With the filtrate analyzed for total S (TS) by inductively coupled plasma–optical emission spectrometry (ICP–OES, iCAP 6500, Thermofisher Scientific), total N (TN), and C_{org} using Shimadzu TOC-VCPH analyzer (Shimadzu Corporation). Furthermore, SO_4^{2-} was measured by ion chromatography (Dionex ICS-3000, Thermo-Fisher Scientific), whereas NO_3^- and NH_4^+ were determined via continuous flow analysis (CFA Analyzer

FLOWSYS 3-Kanal, Alliance Instruments). Due to a lower capacity of the laboratory, not all samples of the March event could be analyzed; therefore, a subselection of representative samples was made. Total P (TP) was measured in the filtrates and also in untreated water samples with an inductively coupled plasma–mass spectrometry (ICP–MS, Agilent 7900 ICP-MS, Agilent Technologies). Colloids were separated by using asymmetric-flow field flow fraction (AF4), which is a method used to separate particles on basis of their particle size. By coupling the AF4 (Postnova Analytics) online to an ICP-MS (Agilent 7700, Agilent Technologies), the elemental composition of various particle size fractions can be determined. The AF4 settings in this study were identical to those described in Gottselig, Amelung et al. (2017). Three particle size fractions were detected in line with (Gottselig, Amelung et al., 2017): a first fraction ranging from >1 kDa to 20 nm, a second fraction between >20 to 60 nm, and a third fraction >60 nm. For the analysis of N and S fractions, a filtration cascade was applied. To elucidate the role of colloids (1–0.1 μm) and nanoparticles (>0.1 μm) for N and S binding and transport more closely, subsamples of the spring event were filtered at 1 μm and at 0.1 μm and analyzed for TS and TN, and the samples of the winter event could not be analyzed due to a lower capacity of the laboratory.

Aliquots of the samples were taken and filtered at 0.45 μm, and any inorganic C in the samples was removed by acidification to pH 1.9 with 37% HCl. This procedure was also applied to blanks and two standard IAEA-CH6 (^{13}C sucrose) and IAEA-600 (^{13}C caffeine.) The ^{13}C values of the total organic C (TOC) in these solute samples were analyzed as $^{13}C_{DOM}$ using a high temperature ISO-TOC cube (Elementar) coupled to a continuous-flow isotope ratio mass spectrometer (Isoprime 100, Elementar) according to the methods of Federherr et al. (2014), Kirkels, et al. (2014), and Leinemann et al. (2018). To keep the possible carryover effects from injection of the syringe to a minimum, only the three last measurements out of five analytical replicate analysis of each sample were used. The observed and expected values of the two standards were calibrated to VPDB (Vienna Pee Dee Belemnite ^{13}C).

These $^{13}C_{DOM}$ values were then compared with the average ^{13}C values of soil organic matter (C_{SOM}) from different soil horizons from the same catchment. In a sampling campaign in 2013 (Gottselig, Wiekenkamp et al., 2017), the litter and fermentation layer of the organic horizon, and the humus layer of the organic horizon, A horizon, and B horizon were sampled at 150 points in the catchment, excluding the Histosols and half-bogs (Gottselig, Wiekenkamp et al., 2017). Freeze-dried and milled samples were analyzed for TOC content and ^{13}C by combustion at 1,080 ˚C in an elemental analyzer (EuroEA, Eurovector) connected to an isotope ratio mass spectrometer (IMRS) (Isoprime, Micromass). The TOC contents were determined by peak integration as well

as calibration against elemental standards. Calibrated laboratory standards were used to ensure the quality of analyses and to scale the raw values to the isotopic reference VPDB. The general precision of replicate analyses is estimated to be better than 5% (relatively) for C content and <0.1‰ for $\delta^{13}C_{org}$. To be able to compare the samples of the catchment outlet, the $^{13}C_{SOM}$ values were averaged over all sampling points per horizon.

2.4 | Data analysis

To compare the nitrate and ammonium concentrations to TN, N-NO$_3^-$, N-NH$_4^+$, and organic N (N$_{org}$) were calculated by performing a mass-based correction. In accordance, comparable corrections were used for sulfate (S-SO$_4^{2-}$, S$_{org}$) to compare with TS.

For the additional analysis of TN and TS concentrations in colloids and nanoparticles of the May event, the untreated samples and the filtrates reflected the following fractions: >1, <1–0.1 (= colloids), and <0.1 μm (1–100 nm = nanoparticles).

Per species, except for δ_{13}C, the concentration − discharge (cQ) relationships were investigated using the approach of Musolff et al. (2015). The relationship between the concentration and discharge could be explained by a power law:

$$C = aQ^b \quad (1)$$

This equation has been rewritten to Equation 2, where W is an error term in case $Q = 0$ and γ is a constant. C, Q, and W are supposed to follow a log-normal distribution:

$$\ln(C) = \ln(a) + b\ln(Q) + \gamma\ln(W) \quad (2)$$

In our dataset, $Q > 0$, and therefore no error term was applied, the equation was as follows:

$$C = a + bQ \quad (3)$$

The b indicates the relationship between C and Q and a as the intercept, and a chemical species with a b slope between −0.1 and 0.1 is considered chemostatic (Herndon et al., 2015). The b was then analyzed together with the ratio of the coefficients of variation of C and Q in the form of Equation 4:

$$\frac{CV_C}{CV_Q} \quad (4)$$

A CV_C that is a lot smaller than CV_Q ($CV_C/CV_Q << 1$) is considered chemostatic (Musolff et al., 2015).

3 | RESULTS

3.1 | Speciation of N and S during the high-precipitation events

The TN, TS, N-NO$_3^-$, and S-SO$_4^{2-}$ concentrations showed a negative relationship with discharge in the winter event (Supplemental Table S2) and decreased during peak flow compared to baseflow (Figure 1a and 1b). The N$_{org}$ and N-NH$_4^+$ concentrations were low (0.05 and 0 mg L^{-1}) during base flow but increased during high flow compared with base flow (maximum concentrations: 0.09 and 0.36 mg L^{-1}), both showed a positive relationship with discharge. Overall, measured TS concentrations were lower than the SO$_4^{2-}$ concentrations detected by a different method; therefore, S-DOS could not be defined for the event in March. We assumed that S$_{org}$ concentrations were low (<0.01 mg L^{-1}) during this event. The R^2 values for the concentrations and the discharge were all lower than 0.7, explaining the variation of concentration in a weak to moderate way.

During the spring event, the log-log relationships of TN, TS, N-NO$_3^-$, and S-SO$_4^{2-}$ were negative with the discharge and showed a decrease during high flow compared with baseflow (Figures 1c and 1d). The N$_{org}$ and S$_{org}$ showed an enrichment over the event, having a positive relationship with the discharge N-NH$_4^+$ concentrations were below detection limit (0.05 mg L^{-1}), except for the moment that the discharge increased (maximum concentration: 0.09 mg L^{-1}), and had a positive log-log relationship with discharge. The relationships between the concentrations of N species and the discharge were weak (TN, N-NH$_4^+$) to moderate (N-NO$_3^-$, N-N$_{org}$), explaining the variations with the highest R^2 of .62. The R^2 of TS and S-SO$_4^2$ were higher, respectively, .7 and .9, and the R^2 of the relationship between S-S$_{org}$ was low.

Concentrations of TN, TS, N-NO$_3^-$, and S-SO$_4^{2-}$ were lower in May than in March, but concentrations of N$_{org}$ and S$_{org}$ were higher. The N-NH$_4^+$ concentrations were similar for both events. The dominance of N-NO$_3^-$ and S-SO$_4^{2-}$ decreased for both events during peak discharge compared with baseflow, and this decrease was most profound during the event in May. The decrease in dominance of N-NO$_3^-$ and S-SO$_4^{2-}$ in the two events was larger for N than for S. The total export of N and S during peak discharge (14 h) was, respectively, 1.23 and 10.03 g in March and 0.37 and 1.09 g in May. TheTN, TS, and S-SO$_4^{2-}$ had similar b values in the cQ relationship during both events, and the b value for N-NO$_3^-$ was larger in May than in March (−0.40 and −0.18, respectively). The N-NH$_4^+$ had a higher positive relationship with discharge in winter than in spring (0.46 and 0.4, respectively). The N-N$_{org}$ had a higher positive relationship with discharge in spring than in winter, with b values equaling 0.61 and 0.21. For all species of N and S, the b values
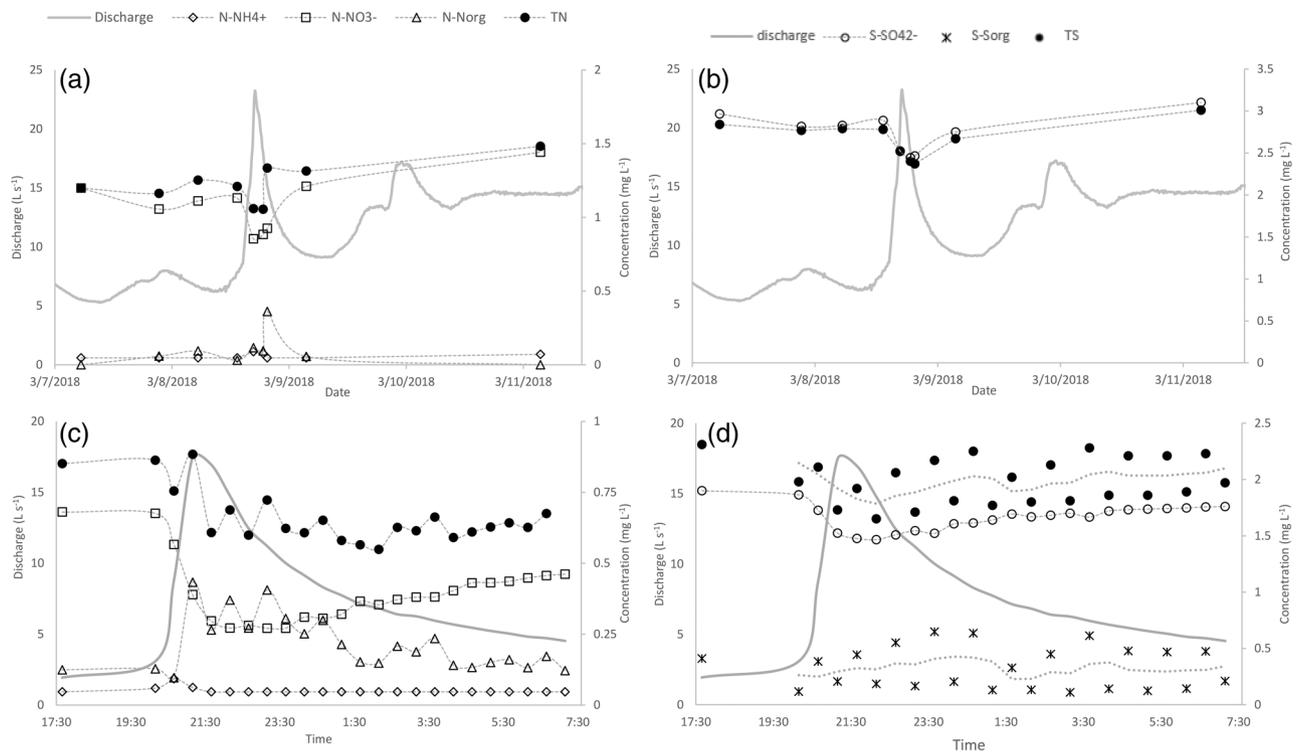
FIGURE 1   Response of (a) N and (b) S species concentrations to a late winter snowmelt and precipitation event in March 2018. Response of (c) N and (d) S species concentrations to a spring precipitation event in May 2018. TN, total N; N_{org}, organic N; TS, total S; S_{org}, organic S

were similar or closer to 0 in spring than in winter, except from, $N\text{-}NO_3^-$, which became more negative, and $N\text{-}N_{org}$, which became more positive. The CV_C/CV_Q values showed the reactivity of the species. The $N\text{-}NH_4^+$ and $N\text{-}N_{org}$ had the highest CV_C/CV_Q values in winter, compared with $N\text{-}NO_3^-$ and $N\text{-}N_{org}$ being the highest in spring. The CV_C/CV_Q values were similar or lower in spring than in winter, except for the CV_C/CV_Q value of $N\text{-}NO_3^-$, which showed a slight increase.

3.2 | Event-based stream water organic C trends

During the winter event, stream water C_{org} concentrations prior to the combined precipitation and snowmelt peak at 1700 h CET of 8 March were, on average, 3.0 ± 0.5 mg L^{-1}, with an export flux of 20.5 mg s^{-1}. Prior to the spring event, C_{org} concentrations were 5.9 mg L^{-1} with similar (5.8 ± 0.2 mg L^{-1}) concentrations during the initial phase of the discharge increase and the export equaled 11.4 mg s^{-1} (Supplemental Figure S3A). In winter, the highest C_{org} concentration (5.8 mg L^{-1}) in the stream water was captured 2.7 h on the falling limb of the hydrograph, with an export of 82.8 mg s^{-1}. After peak flow, the average C_{org} concentration was similar to prior to the precipitation event with 3.2 ± 0.5 mg L^{-1}, but with 44.4 mg s^{-1}, the export

rate was higher than before peak discharge. At maximum measured discharge in spring (17.5 L s^{-1}), C_{org} increased to 10.0 mg L^{-1} with an export of 174.0 mg s^{-1}. The highest C_{org} concentration (11.7 mg L^{-1}) was measured ~1.8 h after peak discharge (Supplemental Figure S3B) and had an export of 130.8 mg s^{-1}. After peak flow C_{org} concentrations decreased to 8.1 ± 0.2 mg L^{-1} but were still higher than during base flow, with 48.0 mg s^{-1}, export was higher as well. The relationship between C_{org} concentrations and discharge was stronger in May than in March, with b values of 0.34 and 0.24, respectively, and had a higher R^2 value in May (Supplemental Table S2). The ratio of variation between discharge and concentration was lower in lower in May than in March, equaling 0.41 and 0.61, respectively.

The $\delta^{13}C_{DOM}$ signal of the March (snowmelt) event was initially $-26.8‰$ but decreased rapidly shortly after precipitation set in Figure 2a, dropping down to a minimum of around $-30.0‰$. However, after the precipitation and snowmelt induced discharge peak, the $\delta^{13}C_{DOM}$ value remained below $-28.0‰$. For the May (rainfall) event, the initial $\delta^{13}C_{DOM}$ value of around $-27.2‰$ quickly dropped to $-27.5‰$ as discharge increased (Figure 2b), but then rapidly increase again as discharge peaked. Approximately 2.5 h after peak discharge, maximum $\delta^{13}C_{DOM}$ values of approximately $-27.1‰$ were reached, which thereafter drop again to $-27.5‰$ during discharge tailing (Figure 2b). In comparison, the
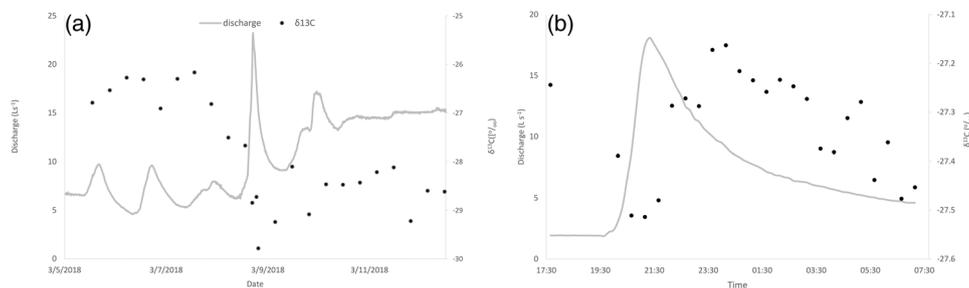
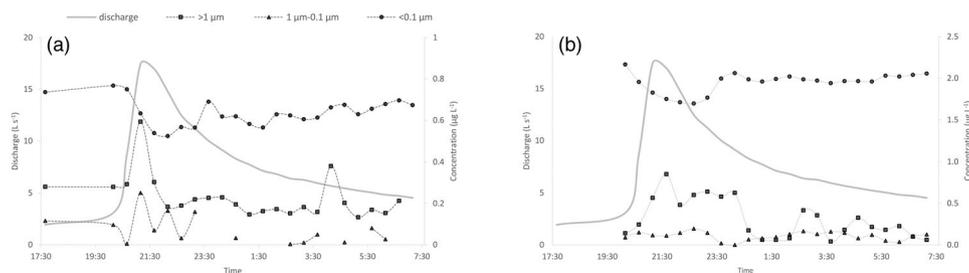**FIGURE 2** δ¹³C value of stream water organic C in (a) March and (b) May event

FIGURE 3 Response of (a) total N and (b) total S concentrations to a spring storm event in May 2018, separated by particle size class

March δ¹³C$_{DOM}$ values fluctuated between −26.2 and −29.8‰, and between −27.2 and −27.5‰ in May.

Compared with measured δ¹³C$_{DOM}$ in stream water, the average organic matter δ¹³C$_{SOM}$ values of the litter + Of horizon, Oh horizon, A horizon, and B horizon in the Wüstebach catchment are −28.4‰ (±0.7), −27.3‰ (±0.5), 27.0‰ (±0.5), and −26.8‰ (±0.6), respectively.

3.3 | Colloidal size fractions during the high-precipitation events

3.3.1 | N, S, and P

The smallest filtration step, <0.1 μm, the nanoparticles, and "truly dissolved" N and S species, showed a slightly negative relationship with discharge (Supplemental Table S2) and decreased during peak flow (Figure 3a and 3b). The larger particulates (>1 μm) and the fine colloid fraction (0.1–1 μm) of N and S showed a positive relationship with discharge. For N, fine colloid fraction (0.1–1 μm) showed the strongest positive relationship and the highest CV$_C$/CV$_Q$ values, which was the case for the larger particulate fraction for S. The R^2 values were highest for the smallest fraction of N and the largest fraction of S, and for the other fractions, R^2 was low. Most of the N and S measured in the samples was of the smallest fraction (<0.1 μm, Figure 3a and 3b), this accounted for 71.5 and 86.3%, respectively, on average during the event. During peak discharge, the smallest fraction (<0.1 μm) was less

dominant. For N, the concentration of the smallest fraction was nearly equal to the concentration of the largest fraction. In this moment, the percentages of the filtration steps were 40.1% (>1 μm), 17.0% (1–0.1 μm), and 42.9% (<0.1 μm). For S, the largest fraction still had the highest concentrations (Figure 3b). The relative contribution to S export during peak discharge was 27.9, 5.43, and 66.7% for the >1-μm fraction, the 1- to 0.1-μm fraction, and the <0.1-μm fraction, respectively.

For the March event, P showed the highest concentrations during peak discharge for all three colloid fractions (Figure 4a). The first fraction (>1 kDa–20 nm) responded strongest to the event with an almost fourfold increase (baseflow: 0.05 μg L^{-1}, peak flow: 0.2 μg L^{-1}), had the strongest positive relationship with discharge and highest CV$_C$/CV$_Q$ values of all fractions, and R^2 were low (Supplemental Table S2). The second fraction (>20–60 nm) gained importance during peak flow with concentrations close to those of the third fraction (second: 0.9 μg L^{-1}, third: 1.0 μg L^{-1}). However, for all samples, most P was transported in the third fraction (>60 nm) (baseflow: 0.65 μg L^{-1}, peak flow: 1.0 μg L^{-1}). After peak discharge, second and third fraction concentrations slowly decreased to a minimum in approximately 4 d. This minimum was similar to the initial values prior to the combined snowmelt/precipitation event. In contrast, the first fraction P concentrations quickly responded to increased discharge and reverted to prior conditions equally fast (Figure 4a). The total P export calculated during peak discharge (14 h) was 4.27 g in March.
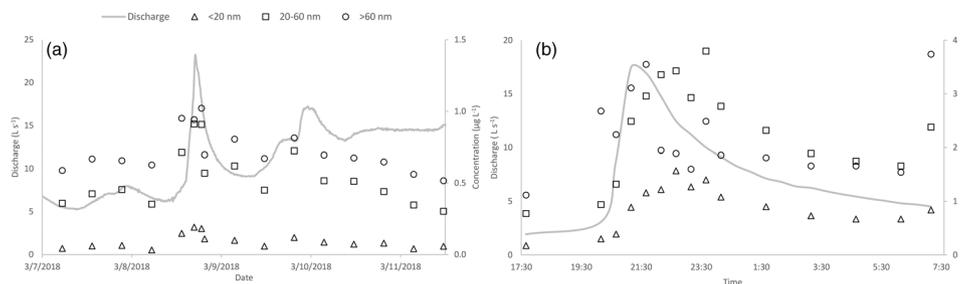
FIGURE 4 Variation of P concentration within the three fractions during the (a) March and (b) May event

In May, the total P export calculated during peak discharge (14 h) was 0.61 g. Additionally, the response to increasing discharge at the beginning of the event varied between the fractions. First fraction P concentrations showed a local maximum during high flow of 1.4 µg L^{-1} and were constantly lower than second and third fraction concentrations (Figure 4b). The second fraction showed the greatest increase in concentration (+2.6 µg L^{-1}). Most P was found in the third fraction during baseflow conditions prior to the precipitation event. This switched shortly after peak discharge to a dominance of P in the second fraction. Concentrations of both the second and third fraction converged again a few hours after peak discharge (Figure 4b). The first fraction showed the strongest positive relationship with discharge and the highest CV_C/CV_Q values of all values. The R^2 values were weak to moderate for the three fractions.

Next to the changes in concentrations during discharge conditions, the relative proportion of P in the three fractions compared with the total P concentration varied as well. For the March event, <6% of total P in the autosampler samples was found in the colloids, with a maximum of 5.9% during peak discharge (Supplemental Figure S4A). In contrast, during the May event, colloidal P accounted for at least 29.5% of total P, with a trend maximum of 63.9% (Supplemental Figure S4B). Also, colloidal P showed more relative variation than during the March event (9.8 ± 3.6 µg L^{-1}). In May the b values indicated a stronger positive relationship between all separate fractions and discharge, which was the most profound in the first and second fraction. For the first and second fraction CV_C/CV_Q values were smaller in the in May than in March, but similar for the third fraction.

3.3.2 | Al and Fe

Concentrations of colloidal Al and Fe also showed an increase from baseflow to peak flow in both March and May events (Supplemental Table S3). In both events, this increase was strongest for the first fraction (approximately four- to ninefold), followed by the second and third fractions. Pearson correlations were calculated for total colloidal P

with total colloidal Fe and Al, based on the sum of the three colloidal fractions (Supplemental Table S4). This reflected the potential building block structures of the colloidal fractions for the transport of P. For the first and second fraction, correlation coefficients were higher for the May (.8–1.0) than for the March (.7–.8) event. However, for the third fraction, coefficients were approximately .1 for Fe and Al in May in contrast with .8 (Al) and .4 (Fe) in March. When looking at the overall correlations, here also calculated for C_{org}, no substantial differences were detected for Fe and Al to P in March and May, yet C_{org} in March correlated less (.1) to P than in May (.7).

4 | DISCUSSION

4.1 | N and S speciation during the events

The negative cQ slope of the S-SO_4^{2-} and N-NO_3^- concentrations and the discharge during both events indicate that the groundwater that normally transports S-SO_4^{2-} and N-NO_3^- is diluted during high flow. This is derived from the study of Weigand et al. (2017), who found that the groundwater-driven tributaries in the Wüstebach catchment showed high solute concentrations. Evans and Davies (1998) described a model where the dilution effect is caused by a relative decrease of the contribution of the groundwater to the discharge due to the relative increase of the contribution of water flowing through organic soil horizons and overland flow. Negative cQ slopes for S-SO_4^{2-} and N-NO_3^- and dilution behavior during events were also found by Knapp et al. (2020) in catchments in the Swiss Alps. Long-term data confirmed the chemostatic and dilution behavior of S-SO_4^{2-} and showed a more chemodynamic relationship but positive cQ slope between N-NO_3^-, although the cQ slopes of N-NO_3^- and discharge were influenced by the type of land use (Musolff et al., 2015). Differences in cQ relationships between the long term and during events and between events were found to be attributed to antecedent wetness and the event characteristics, such as precipitation intensity, temperature, and event duration (Knapp et al., 2020). Concentration discharge relationships

are often used to study long-term effects (Musolff et al., 2015) but can also be used to describe events, using high-resolution data of many events (Knapp et al., 2020). In this study, the number of data that the relationships are based on is relatively low; therefore, R^2 values of the cQ relationships had only low to moderate explanatory power, especially during the March event. However, the cQ relationships can still be used to help understand the dynamics of nutrient export of these two events, as they support the trends we observe based on the concentration and export dynamics.

In May, the cQ slope of $N-NO_3^-$ and discharge was more negative, indicating a stronger dilution effect, which is in line with the findings of Gao et al. (2014) and Inamdar et al. (2006). The cQ slope of $S-SO_4^{2-}$ were slightly more negative in May but would still count as chemostatic (Herndon et al., 2015). This could be attributed to higher inter event variability of the cQ slope for $N-NO_3^-$ and the cQ slope of $S-SO_4^{2-}$ due a higher dependence on the biological activity (Knapp et al., 2020). Both $N-NO_3^-$ and $S-SO_4^{2-}$ export is dependent on the antecedent wetness of the catchment. After dry periods, export of nutrients is low due to low leaching rates, and older water, rich in solutes, is mobilized and gets pushed out; this it called the "old water" effect (Inamdar et al., 2006). High antecedent wetness can make the hillslopes connected to the stream, and in the case of Wüstebach, shallow groundwater then flows from the hillslopes to the riparian zone triggered by pressure waves from the precipitation (Stockinger et al., 2014). On average, the antecedent catchment wetness in the Wüstebach catchment is high during the late autumn to early spring period (i.e., between first of November and first of May; Rosenbaum et al., 2012; Stockinger et al., 2014). However, catchment responses of $N-NO_3^-$ and $S-SO_4^{2-}$ export can be similar when antecedent wetness is low but precipitation intensity and duration are high (Inamdar et al., 2006; Knapp et al., 2020; Stockinger et al., 2014). During the March event, the stream was connected to the hillslopes, as the antecedent wetness of the catchment was high, but this was low in May. Therefore, the lower cQ slope $N-NO_3^-$ in May than in March can be explained by the short duration of the event and low antecedent catchment wetness (Knapp et al., 2020).

The $N-NH_4^+$ concentrations were close to detection limit, but during the rising limb of the hydrograph, the concentrations showed a peak. Usually this peak is also at the same time as the highest intensity in rainfall, which is not necessarily peak flow. This shows that $N-NH_4^+$ export is a surface water-driven process, which was also found by Butturini and Sabater (2002) and Inamdar et al. (2006). In other situations, $N-NH_4^+$ is nitrified quickly by microbes in the water to nitrate or used up directly by plants as a nutrient. During high-intensity rainfall events this nitrification is disrupted by surface water mixing, and $N-NH_4^+$ will be exported (Cooper, 1983); therefore, higher $N-NH_4^+$ concentrations occur dur-

ing events than during baseflow. The S_{org} in May and N_{org} showed the same response as $N-NH_4^+$, responding strongly to rainfall to the increase in discharge. Concentrations of biologically associated solutes and particulates, such as (dissolved) C_{org}, including N_{org} and S_{org}, show increased export during high flow of HD events. This a surface water-driven process, caused by overland flow and water flowing through organic horizons and mineral soil horizons at the surface (David & Mitchell, 1987; Inamdar & Mitchell, 2007; Inamdar et al., 2006; Rose et al., 2018). The driver behind the high concentration of N_{org} and S_{org} could also be explained by preferential flow paths in the top soil that are active during the dry season (Wiekenkamp et al., 2016) and transporting these species to the Wüstebach stream from the topsoil and surface (Weigand et al., 2017).

The N_{org}, $N-NH_4^+$, and S_{org} did show the opposite behavior of $N-NO_3^-$ and $S-SO_4^{2-}$, as they showed a positive relationship with discharge, having their maximum when the discharge was also at its maximum (Inamdar & Mitchell, 2007; Rose et al., 2018). The study by Gao et al. (2014) also shows that during peak discharge, the diversity of N species increases, having more particulate N and N_{org} during peak discharge and less nitrate. Indeed, during the two events with the highest intensity, 59.4 and 32.2 mm, the diversity of N species was the largest and showed a peak in TN, due to large particulate N transport (Gao et al., 2014). In contrast, in an event with 19.8 mm precipitation, the TN and N species showed a dilution effect (Gao et al., 2014). Therefore, N diversity and probably S diversity, as they have similar drivers (Inamdar et al., 2006), increase with higher precipitation intensity, causing a peak in TN, but a dilution effect in nitrate concentrations. Gao et al. (2014) were only focusing on summer events in July and August, and therefore the events show larger diversity of N species. The N_{org} and S_{org} concentrations in our study were both higher in spring than in winter due to the decrease of vegetation and biological activity in winter, S_{org} concentrations were even negligible during winter, and N and S specification diversity is lower. These organic species are usually strongly affected by seasonality (Knapp et al., 2020), their abundance in May could be attributed to changes soil and pore water chemistry due to higher temperature (Clark et al., 2004). Another reason for the lower N_{org} and S_{org} concentrations could be that overland flow is not occurring as often during snowmelt events as during rainfall events due to infiltrating snowmelt water and the higher groundwater table, which can also be on top of a frozen soil layer (Laudon et al., 2004). Overall, more N and S was exported in total in March than in May, the reason behind this was that the total N export during peak discharge was 3.3-fold higher in March than in May, and the total S export during peak discharge was 9.2-fold higher in March than in May (Supplemental Table S1). This is due to higher discharge, of which more was influenced by interflow and shallow groundwater flow due to hydrological

connectivity and higher concentrations of N and S because of lower microbial activity. In May, overland flow and water flowing through organic horizons played a larger role than in March, shown by the lower dominance of N-NO_3^- and S-SO_4^{2-} compared with N_{org} and S_{org}.

4.2 | Event-based organic C signatures and coupling to other elements

The overall response of C_{org} export due to increasing discharge was comparable for both events, but with a slightly higher rate of increase in March (factor of 1.9 vs. 1.7), but precipitation amounts in March were lower than in May. However, snowmelt has the potential to mobilize C_{org} in forest ecosystems, and thus the increased stream waters concentrations can occur despite the normal situation of an overall low C_{org} concentrations in colder seasons, because the large amount of water from snowmelt can flow through soil horizons rich in organic material (Boyer et al., 1997; Sebestyen et al., 2009). Longer periods of snow cover may even trigger large C_{org} responses due to continuing microbial activity beneath the snow cover, as the temperature can be higher than at the soil surface (Hornberger et al., 1994). Evidently, baseflow C_{org} concentrations were higher before the May event, and the response time (until maximum C_{org} export) was reached 0.9 h faster than for the March event. This difference can also be attributed to the slower wetting of the soil through the thawing of the snow, compared with the direct precipitation in the May event. The faster activation of preferential flow paths could also play a role during this event and export of C_{org} from the saturated riparian zone, compared with a slower response from the whole catchment governed by hydrological connectivity in winter (Bogena et al., 2013; Stockinger et al., 2014; Wiekenkamp et al., 2016). Despite the quicker export during the May event, maximum C_{org} export was reached with a delay time of 1.8 h after peak discharge. This can either be due to a rainwater dilution effect or the longer travel time of the C_{org} derived from the half-bogs and Histosols in the area to the catchment outlet, these areas function as C_{org} hotspots (Grabs et al., 2012; Lambert et al., 2011). In March, the delay in maximum C_{org} export can be explained by the longer travel time of C_{org} derived from the hydrologically connected hillslopes. Here, the water present in the riparian zone is pushed out by the pressure wave created when precipitation falling on the entire catchment travels through the soil and then reaches the riparian zone (Stockinger et al., 2014). The water that is "pushed out" of the riparian zone is assumed to be enriched in C_{org} (Tunaley et al., 2016), especially so when water moves through organic soils surrounding boreal or upland streams (Grabs et al., 2012; Laudon et al., 2011).

The differences in catchment response caused by the co-occurrence of snowmelt and rainfall compared with rainfall alone, leading to a larger influence surface water, and superficial terrestrial C inputs for the event in May could also potentially be confirmed by the δ^{13}C signal (Figure 2). Despite the fact that δ^{13}C screening is not as specific to assess terrestrial organic matter as, for example, measurement of lignin phenols, the stable carbon isotope composition still differs throughout the soil profile (Lambert et al., 2011; Onstad et al., 2000). The $\delta^{13}C_{SOM}$ values from organic soil horizons are generally substantially lower (i.e., more depleted in ^{13}C content) relative to mineral and lower soil horizons (Cole et al., 2002; Lambert et al., 2011; Mook & Tan, 1991). This is corroborated by our own measurements in the Wüstebach catchment revealing about 1.5‰ difference between organic and mineral soil horizons. Therefore, the switch (first heavier, then lighter than −28.0‰) in the $\delta^{13}C_{DOM}$ signal observed for the March event can be explained by a change from mineral soil horizons sources prior to the precipitation to organic soil horizons post peak discharge. This means that before the precipitation event, only snowmelt was causing runoff. Interflow and shallow groundwater export C_{org} from the mineral soil layers within the whole catchment, due to hydrological connectivity (Stockinger et al., 2014). This changes due to the precipitation, which causes the horizons rich in organic material to react and C_{org} is lost from the topsoil from largely the riparian zone during and after the precipitation. It can be seen from the low C_{org} concentrations before peak discharge that organic C mobilization occurs under the snow cover (Hornberger et al., 1994), but at a slower rate than when it rains. The same phenomenon has also been described by Lambert et al. (2011), where $\delta^{13}C_{DOM}$ values drop during peak discharge due to a change from base flow to storm flow, inducing overland flow and flow of water through organic horizons, making the saturated peatland the main C_{org} export mechanism, being coupled to the export of N_{org} and S_{org}.

4.3 | Event-based transport of colloidal N, S, and P fractions

During the precipitation event (May 2018) most of the colloidal S and N (<1 μm) was present within the nanoparticle fraction size (<0.1 μm). This fraction showed similar behavior to the inorganic ions, decreasing during peak discharge, and increasing after; thus, they likely represented the NO_3^- and SO_4^{2-} ions. Note the truly dissolved fraction could not be analytically isolated from the nanoparticles for N and S. For N and S in second largest (particulates >1 μm) and in N in the lowest (colloids 0.1–1 μm) proportional fraction, they exhibit a similar behavior to the N_{org} and S_{org}, having a maximum coinciding with discharge and a positive cQ slope. The S present in the colloids showed little response to the increase in discharge, only being slightly larger during peak discharge than during baseflow. The precise chemical composition of

N_{org} and S_{org} was not investigated in our study but could, for example, be amino acids, SO_4^{2-} esters, and SO_4^{2-} particles and connected to iron and aluminum ions (Gottselig et al., 2014; Scherer, 2009).

Total P export during peak discharge was 7.0-fold higher in March than in May. However, relatively more P was transported bound to NNP during the May event than in March. This percentage of NNP was ~50% during the May discharge even, but only around 3% in March. Evidently, more P was transported and recycled in riparian area near stream in May than in March, which also seems to be crucial for the colloidal stream P concentrations. Influential factors for the low colloidal binding could be the equally lower C_{org} and Fe export, as they have been described as primary binding partners of P in ecosystems (Gottselig, Nischwitz et al., 2017; Regelink et al., 2013; Stolpe et al., 2013). Correlations between the Al, Fe, C_{org}, and P data indicate potential coupled export processes. Evidently, C_{org} and P (correlation coefficient = .1) were not found to be transported similarly during the combined snowmelt and precipitation event in March. Despite the mobilization potential of snow cover for C_{org} (Boyer et al., 1997; Sebestyen et al., 2009) concentrations were seemingly too low for substantial P transport capacities. In contrast, this situation was far more likely for the May event ($r\check{s}$ = .7), a finding that confirms the general assumption that C_{org} is a relevant binding partner for P in colloids (Darch et al., 2014; Regelink et al., 2013) and even has the potential to stabilize colloids (Ranville & Macalady, 1996; Six et al., 1999). The specific role of C_{org} for the individual fractions could not be resolved in this study, yet due to the siliceous bedrock in Wüstebach and evidence from previous studies (Gottselig, Amelung et al., 2017; Gottselig, Nischwitz et al., 2017), it can be assumed that the role of C_{org} in May was predominantly for P binding within the third fraction (>60 nm). Next to C_{org}, combinations of Fe and C_{org} as well as metals and clay minerals were previously identified as primary building blocks for different fractions of P containing colloids (Gottselig, Nischwitz et al., 2017). Of these, only third-fraction data differ from literature findings, with a stark contrast also between March and May. It can therefore be assumed that this fraction shows highest variability between baseflow and peak discharge conditions, as well as between winter and spring events. Potentially, third-fraction particles (size range > 60 nm) are mobilized and translocated differently than smaller nanoparticles (first and second fraction, >1 kDa–20 nm and >20–60 nm) during events in general and specifically when typical short spring events take place, like in May. However, the first-fraction particles showed the strongest positive cQ relationship and the highest CV_C/CV_Q values, which explains their mobility.

It was found that the export of P and in smaller amounts N and S via nondissolved pathways take place more often during rainfall events than combined snowmelt and rainfall events. With the increase of rainfall events, this way of nutrient export will be more common in the future, which makes it harder to quantify a large part of the export of P and parts of the export of N and S.

5 | CONCLUSIONS

Stream water $\delta^{13}C$ data highlighted that the Wüstebach catchment did not return to pre-baseline conditions after a 2-d March snowmelt, in contrast with the shorter (several hours) May precipitation event, indicating a more significant effect of the winter event on N, S, P, and C_{org} export, likely due to its longer duration. However, there were substantial effects for both events on total and specification of N, S, P, and C_{org}. Colloidal export contributed <6% of total stream water P in March, but 29–64% in May, and was then more strongly correlated to C_{org} exports, suggesting an increased role of overland flow and subsurface flow through organic soil horizons. Colloidal NH_4^+ and N_{org} (>0.1 µm) and particulate S_{org} (>1 µm) were higher during both events, but the majority of losses were still as dissolved $N-NO_3^-$ and $S-SO_4^{2-}$. This dominance was larger in late winter than spring, due to decreased biological activity and more groundwater influence through high antecedent catchment wetness. Since high-intensity or longer-duration precipitation events are predicted to occur more frequently due to climate change, such weather-driven catchment nutrient losses may therefore simultaneously increase. This study highlights the often underreported role of particulates, colloids, and nanoparticles within biogeochemical cycles and the need for better quantification of such solid fractions and associated nutrient species.

AUTHOR CONTRIBUTIONS
Dymphie J. Burger: Data curation; Formal analysis; Investigation; Writing-original draft. Johnny Vogel: Data curation; Formal analysis; Investigation; Writing-original draft. Roland Bol: Project administration; Supervision; Writing-review & editing. Annemieke M. Kooijman: Supervision; Writing-review & editing. Eva de Rijke: Investigation; Resources. Jorien Schoorl: Investigation; Resources. Andreas

Lücke: Writing-review & editing; Data Curation. Nina Gottselig: Investigation; Project administration; Supervision; Writing-review & editing.

CONFLICT OF INTEREST

The authors declare that there was no conflict of interest.

DATA AVAILABILITY STATEMENT

Climate and hydrological data, as well as data on TN and C_{org} (DOC) concentrations, are publicly available on the TERENO platform (http://www.tereno.net/ddp/). The other data used in this study are available from the corresponding author on request.

ORCID

Dymphie J. Burger https://orcid.org/0000-0002-8773-3578

Annemieke M. Kooijman https://orcid.org/0000-0001-9177-632X

Roland Bol https://orcid.org/0000-0003-3015-7706

Eva de Rijke https://orcid.org/0000-0002-9341-6501

Andreas Lücke https://orcid.org/0000-0003-4199-0808

REFERENCES

Bogena, H. R., Bol, R., Borchard, N., Brüggeman, N., Diekkrüger, B., Drüe, C., Groh, J., Gottselig, N., Huisman, J. A., Lücke, A., Missong, A., Neuwirth, B., Pütz, T., Schmidt, M., Stockinger, M., Tappe, W., Weihermüller, L., Wiekenkamp, I., & Vereecken, H. (2015). A terrestrial observatory approach to the integrated investigation of the effects of deforestation on water, energy, and matter fluxes. *Science China Earth Sciences*, *58*, 61–75. https://doi.org/10.1007/s11430-014-4911-7

Bogena, H. R., Herbst, M., Huisman, J. A., Rosenbaum, U., Weuthern, A., & Vereecken, H. (2010). Potential of wireless sensor networks for measuring soil water content variability. *Vadose Zone Journal*, *9*, 1002–1013. https://doi.org/10.2136/vzj2009.0173

Bogena, H. R., Huisman, J. A., Baatz, R., Hendricks Franssen, H. J., & Vereecken, H. (2013). Accuracy of the cosmic-ray soil water content probe in humid forest ecosystems: The worst case scenario. *Water Resources Research*, *49*, 5778–5791. https://doi.org/10.1002/wrcr.20463

Bogena, H. R., Montzka, C., Huisman, J. A., Graf, A., Schmidt, M., Stockinger, M., von Hebel, C., Hendricks Franssen, H. J., van der Kruk, J., Tappe, W., Lücke, A., Baatz, R., Bol, R., Groh, J., Pütz, T., Jakobi, J., Kunkel, R., Sorg, J., & Vereecken, H. (2018). The TERENO-Rur hydrological observatory: A multiscale multi-compartment research platform for the advancement of hydrological science. *Vadose Zone Journal*, *17*(1). https://doi.org/10.2136/vzj2018.03.0055

Bol, R., Julich, D., Brödlin, D., Siemens, J., Kaiser, K., Dippold, M. A., Spielvogel, S., Zilla, T., Mewes, D., Blanckenburg, F. von, Puhlmann, H., Holzmann, S., Weiler, M., Amelung, W., Lang, F., Kuzyakov, Y., Feger, K. H., Gottselig, N., Klumpp, E., … Hagedorn, F. (2016). Dissolved and colloidal phosphorus fluxes in forest ecosystems: An almost blind spot in ecosystem research. *Journal of Plant Nutri-*

tion and Soil Science, *179*, 425–438. https://doi.org/10.1002/jpln.201600079

Bol, R., Lücke, A., Tappe, W., Kummer, S., Krause, M., Weigand, S., Pütz, T., & Vereecken, H. (2015). Spatio-temporal variations of dissolved organic matter in a German forested mountainous headwater catchment. *Vadose Zone Journal*, *14*(4). https://doi.org/10.2136/vzj2015.01.0005

Boyer, E. W., Hornberger, G. M., Bencala, K. E., & McKnight, D. M. (1997). Response characteristics of DOC flushing in an alpine catchment. *Hydrological Processes*, *11*, 1635–1647. https://doi.org/10.1002/(SICI)1099-1085(19971015)11:12%3c1635::AID-HYP494%3e3.0.CO;2-H

Brooks, P. D., Williams, M. W., & Schmidt, S. K. (1998). Inorganic nitrogen and microbial biomass dynamics before and during spring snowmelt. *Biogeochemistry*, *43*, 1–15. https://doi.org/10.1023/A:1005947511910

Butturini, A., & Sabater, F. (2002). Nitrogen concentrations in a small Mediterranean stream: 1. Nitrate 2. Ammonium. *Hydrology and Earth System Sciences*, *6*, 539–550. https://doi.org/10.5194/hess-6-539-2002

Clark, M. J., Cresser, M. S., Smart, R., Chapman, P. J., & Edward, A. C. (2004). The influence of catchment characteristics on the seasonality of carbon and nitrogen species concentrations in upland rivers of northern Scotland. *Biogeochemistry*, *68*, 1–19. https://doi.org/10.1023/B:BIOG.0000025733.07568.11

Cole, J. J., Carpenter, S. R., Kitchell, J. F., & Pace, M. L. (2002). Pathways of organic carbon utilization in small lakes: Results from a whole-lake ^{13}C addition and coupled model. *Limnology and Oceanography*, *47*, 1664–1675. https://doi.org/10.4319/lo.2002.47.6.1664

Cole, J. J., Prairie, Y. T., Caraco, N. F., McDowell, W. F., Tranvik, L. J., Striegl, R. G., Duarte, C. M., Kortelainen, P., Downing, J. A., Middelburg, J. J., & Melack, J. (2007). Plumbing the global carbon cycle: Integrating inland waters into the terrestrial carbon budget. *Ecosystems*, *10*, 172–185. https://doi.org/10.1007/s10021-006-9013-8

Cooper, A. B. (1983). Effect of storm events on benthic nitrifying activity. *Applied and Environmental Microbiology*, *46*, 957–960. https://doi.org/10.1128/AEM.46.4.957-960.1983

Crews, T. E., Kitayama, K., Fownes, J. H., Riley, R. H., Herbert, D. A., Mueller-Dombois, D., & Vitousek, P. M. (1995). Changes in soil phosphorus fractions and ecosystem dynamics across a long chronosequence in Hawaii. *Ecology*, *76*, 1407–1424. https://doi.org/10.2307/1938144

Darch, T., Blackwell, M. S., Hawkins, J. M. B., Haygarth, P. M., & Chadwick, D. (2014). A meta-analysis of organic and inorganic phosphorus in organic fertilizers, soils, and water: Implications for water quality. *Critical Reviews in Environmental Science and Technology*, *44*, 2172–2202. https://doi.org/10.1080/10643389.2013.790752

David, M. B., & Mitchell, M. J. (1987). Transformations of organic and inorganic sulfur: Importance to sulfate flux in an Adirondack forest soil. *Japca*, *37*, 39–44. https://doi.org/10.1080/08940630.1987.10466198

Domagalski, J. L., & Johnson, H. M. (2011). Subsurface transport of orthophosphate in five agricultural watersheds, USA. *Journal of Hydrology*, *409*, 157–171. https://doi.org/10.1016/j.jhydrol.2011.08.014

Etmann, M. (2009). *Dendrological recordings in the Wüstebach head water catchment area using various measurement and*

estimation methods (In German, Master's thesis, Westfälische Wilhelms-Universität).

Evans, C., & Davies, T. D. (1998). Causes of concentration/discharge hysteresis and its potential as a tool for analysis of episode hydrochemistry. *Water Resources Research*, *34*, 129–137. https://doi.org/10.1029/97WR01881

Fabre, A., Pinay, G., & Ruffinoni, C. (1996). Seasonal changes in inorganic and organic phosphorus in the soil of a riparian forest. *Biogeochemistry*, *35*, 419–432. https://doi.org/10.1007/BF02183034

Federal German Government. (2015). *Progress report of the German strategy for adaptation to climate change*. (In German.) Federal German Government. https://www.bmu.de/fileadmin/Daten_BMU/Download_PDF/Klimaschutz/klimawandel_das_fortschrittsbericht_bf.pdf

Federherr, E., Cerli, C., Kirkels, F. M. S. A., Kalbitz, K., Kupka, H. J., Dunsbach, R., Lange, L., & Schmidt, T. C. (2014). A novel high-temperature combustion based system for stable isotope analysis of dissolved organic carbon in aqueous samples. I: Development and validation. *Rapid Communications in Mass Spectrometry*, *28*, 2559–2573. https://doi.org/10.1002/rcm.7052

Gao, Y., Zhu, B., Yu, G., Chen, W., He, N., Wang, T., & Miao, C. (2014). Coupled effects of biogeochemical and hydrological processes on C, N, and P export during extreme rainfall events in a purple soil watershed in southwestern china. *Journal of Hydrology*, *511*, 692–702. https://doi.org/10.1016/j.jhydrol.2014.02.005

Gottselig, N., Amelung, W., Kirchner, J. W., Bol, R., Eugster, W., Granger, S. J., Hérnandez-Crespo, C., Herrman, F., Keizer, J. J., Korkiakoski, M., Laudon, H., Lehner, I., Löfgren, S., Lohila, A., MacLeod, C. J. A., Mölder, M., Müller, C., Nasta, P., Nischwitz, V., … Klumpp, E. (2017). Elemental composition of natural nanoparticles and fine colloids in European forest stream waters and their role as phosphorus carriers. *Global Biogeochemical Cycles*, *31*, 1592–1607. https://doi.org/10.1002/2017GB005657

Gottselig, N., Bol, R., Nischwitz, V., Amelung, W., Vereecken, H., & Klumpp, E. (2014). Distribution of phosphorus-containing fine colloids and nanoparticles in stream water of a forest catchment. *Vadose Zone Journal*, *13*(7). https://doi.org/10.2136/vzj2014.01.0005

Gottselig, N., Nischwitz, V., Meyn, T., Amelung, W., Bol, R., Halle, C., Vereecken, H., Siemens, J., & Klumpp, E. (2017). Phosphorus binding to nanoparticles and colloids in forest stream waters. *Vadose Zone Journal*, *16*(3). https://doi.org/10.2136/vzj2016.07.0064

Gottselig, N., Wiekenkamp, I., Weihermüller, L., Brüggeman, N., Berns, A. E., Bogena, H. R., Borchard, N., Klumpp, E., Lücke, A., Missong, A., Pütz, T., Vereecken, H., Huisman, J. A., & Bol, R. (2017). A three-dimensional view on soil biogeochemistry: A dataset for a forested headwater catchment. *Journal of Environmental Quality*, *46*, 210–218. https://doi.org/10.2134/jeq2016.07.0276

Grabs, T., Bishop, K., Laudon, H., Lyon, S. W., & Seibert, J. (2012). Riparian zone hydrology and soil water total organic carbon (TOC): Implications for spatial variability and upscaling of lateral riparian TOC exports. *Biogeosciences*, *9*, 3901–3916. https://doi.org/10.5194/bg-9-3901-2012

Graf, A., Bogena, H. R., Drüe, C., Hardelauf, H., Pütz, T., Heinemann, G., & Vereecken, H. (2014). Spatiotemporal relations between water budget components and soil water content in a forested tributary catchment. *Water Resources Research*, *50*, 4837–4857. https://doi.org/10.1002/2013WR014516

Haygarth, P. M., Hepworth, L., & Jarvis, S. C. (1998). Forms of phosphorus transfer in hydrological pathways from soil under grazed grassland. *Journal of European Soil Science*, *49*, 65–72. https://doi.org/10.1046/j.1365-2389.1998.00131.x

Heathwaite, A. L., Dils, R. M., Liu, S., Carvalho, L., Brazier, R. E., Pope, L., Hughes, M., Philips, G., & May, L. (2005). A tiered risk-based approach for predicting diffuse and point source phosphorus losses in agricultural areas. *Science of the Total Environment*, *344*, 225–239. https://doi.org/10.1016/j.scitotenv.2005.02.034

Herndon, E. M., Dere, A. L., Sullivan, P. L., Norris, D., Reynolds, B., & Brantley, S. L. (2015). Landscape heterogeneity drives contrasting concentration–discharge relationships in shale headwater catchments. *Hydrology and Earth System Sciences*, *19*, 3333–3347. https://doi.org/10.5194/hess-19-3333-2015

Hornberger, G. M., Bencala, K. E., & McKnight, D. M. (1994). Hydrological controls on dissolved organic carbon during snowmelt in the Snake River near Montezuma, Colorado. *Biogeochemistry*, *25*, 147–165. https://doi.org/10.1007/BF00024390

Inamdar, S. P., & Mitchell, M. J. (2007). Storm event exports of dissolved organic nitrogen (DON) across multiple catchments in a glaciated forested watershed. *Journal of Geophysical Research: Biogeosciences*, *112*(G2).

Inamdar, S. P., O'leary, N., Mitchell, M. J., & Riley, J. T. (2006). The impact of storm events on solute exports from a glaciated forested watershed in western New York, USA. *Hydrological Processes: An International Journal*, *20*, 3423–3439. https://doi.org/10.1002/hyp.6141

Inamdar, S. P., Singh, S., Dutta, S., Levia, D., Mitchell, M. J., Scott, D., Bais, H., & MacHale, P. (2011). Fluorescence characteristics and sources of dissolved organic matter for stream water during storm events in a forested mid-Atlantic watershed. *Journal of Geophysical Research: Biogeosciences*, *116*(G3).

Johnson, D. W., & Cole, D. W. (1980). Anion mobility in soils: Relevance to nutrient transport from forest ecosystems. *Environment International*, *3*, 79–90. https://doi.org/10.1016/0160-4120(80)90040-9

Julich, S., Benning, R., Julich, D., & Feger, K. H. (2017). Quantification of phosphorus exports from a small forested headwater-catchment in the eastern Ore Mountains. *Forests*, *8*, 206. https://doi.org/10.3390/f8060206

Kirkels, F. M. S. A., Cerli, C., Federherr, E., Gao, J., & Kalbitz, K. (2014). A novel high-temperature combustion based system for stable isotope analysis of dissolved organic carbon in aqueous samples. II: Optimization and assessment of analytical performance. *Rapid Communications in Mass Spectrometry*, *28*, 2574–2586. https://doi.org/10.1002/rcm.7053

Kleinman, P. J., Srinivasan, M., Dell, C. J., Schmidt, J. P., Sharpley, A. N., & Bryant, R. B. (2006). Role of rainfall intensity and hydrology in nutrient transport via surface runoff. *Journal of Environmental Quality*, *35*, 1248–1259. https://doi.org/10.2134/jeq2006.0015

Knapp, J., Freiin von Freyberg, J., Studer, B., Kiewiet, L., & Kirchner, J. W. (2020). Concentration-discharge relationships vary among hydrological events, reflecting differences in event characteristics. *Hydrology and Earth System Sciences Discussions*. https://doi.org/10.5194/hess-24-2561-2020

Lambert, T., Pierson-Wickmann, A. C., Gruau, G., Thibault, J. N., & Jaffrézic, A. (2011). Carbon isotopes as tracers of dissolved organic carbon sources and water pathways in headwater catchments. *Journal of Hydrology*, *402*, 228–238. https://doi.org/10.1016/j.jhydrol.2011.03.014

Lang, F., Bauhus, J., Frossard, E., George, E., Kaiser, K., Kaupenjohann, M., Krüger, J., Matzner, E., Polle, A., Prietzel, J., Rennenberg,

H., & Wellbrock, N. (2016). Phosphorus in forest ecosystems: New insights from an ecosystem nutrition perspective. *Journal of Plant Nutrition and Soil Science*, *179*, 129–135. https://doi.org/10.1002/jpln.201500541

Laudon, H., Berggren, M., Ågren, A., Buffam, I., Bishop, K., Grabs, T., Jansson, M., & Köhler, S. (2011). Patterns and dynamics of dissolved organic carbon (DOC) in boreal streams: The role of processes, connectivity, and scaling. *Ecosystems*, *14*, 880–893. https://doi.org/10.1007/s10021-011-9452-8

Laudon, H., Seibert, J., Köhler, S., & Bishop, K. (2004). Hydrological flow paths during snowmelt: Congruence between hydrometric measurements and oxygen 18 in meltwater, soil water, and runoff. *Water Resources Research*, *40*(3). https://doi.org/10.1029/2003WR002455

Lead, J. R., & Wilkinson, K. J. (2006). Aquatic colloids and nanoparticles: Current knowledge and future trends. *Environmental Chemistry*, *3*, 159–171. https://doi.org/10.1071/EN06025

Leinemann, T., Preusser, S., Mikutta, R., Kalbitz, K., Cerli, C., Höschen, C., Müller, C. W., Kandeler, E., & Guggenberger, G. (2018). Multiple exchange processes on mineral surfaces control the transport of dissolved organic matter through soil profiles. *Soil Biology and Biochemistry*, *118*, 79–90. https://doi.org/10.1016/j.soilbio.2017.12.006

Martin, J. M., Dai, M. H., & Cauwet, G. (1995). Significance of colloids in the biogeochemical cycling of organic carbon and trace metals in the Venice Lagoon (Italy). *Limnology and Oceanography*, *40*, 119–131. https://doi.org/10.4319/lo.1995.40.1.0119

Mayer, T. D., & Jarrell, W. M. (1995). Assessing colloidal forms of phosphorus and iron in the Tualatin River basin. *Journal of Environmental Quality*, *24*, 1117–1124. https://doi.org/10.2134/jeq1995.00472425002400060010x

McNeill, A., Eriksen, J., Bergström, L., Smith, K. A., Marstrop, H., Kirchmann, H., & Nilsson, I. (2005). Nitrogen and sulphur management: Challenges for organic sources in temperate agricultural systems. *Soil Use and Management*, *21*, 82–93. https://doi.org/10.1079/SUM2005303

Mitchell, M. J., Burke, M. K., & Shepard, J. P. (1992). Seasonal and spatial patterns of S, Ca, and N dynamics of a northern hardwood forest ecosystem. *Biogeochemistry*, *17*, 165–189. https://doi.org/10.1007/BF00004040

Mitchell, M. J., Piatek, K. B., Christopher, S., Mayer, B., Kendall, C., & McHale, P. (2006). Solute sources in stream water during consecutive fall storms in a northern hardwood forest watershed: A combined hydrological, chemical and isotopic approach. *Biogeochemistry*, *78*, 217–246. https://doi.org/10.1007/s10533-005-4277-1

Mook, W. G., & Tan, F. C. (1991). Stable carbon isotopes in rivers and estuaries. In E. T. Degens, S. Kempe, & J. E. Richey (Eds.), *Biogeochemistry of major world rivers* (1st ed., pp. 245–264). John Wiley and Sons.

Musolff, A., Schmidt, C., Selle, B., & Fleckenstein, J. H. (2015). Catchment controls on solute export. *Advances in Water Resources*, *86*, 133–146. https://doi.org/10.1016/j.advwatres.2015.09.026

Neubauer, E., von der Kammer, F., Knorr, K. H., Peiffer, S., Reichert, M., & Hofmann, T. (2013). Colloid-associated export of arsenic in stream water during stormflow events. *Chemical Geology*, *352*, 81–91. https://doi.org/10.1016/j.chemgeo.2013.05.017

Onstad, G. D., Canfield, D. E., Quay, P. D., & Hedges, J. I. (2000). Sources of particulate organic matter in rivers from the continental USA: Lignin phenol and stable carbon isotope compositions. *Geochimica Et Cosmochimica Acta*, *64*, 3539–3546. https://doi.org/10.1016/S0016-7037(00)00451-8

Park, J., Duan, L., Kim, B., Mitchell, M. J., & Shibata, H. (2010). Potential effects of climate change and variability on watershed biogeochemical processes and water quality in northeast Asia. *Environment International*, *36*, 212–225. https://doi.org/10.1016/j.envint.2009.10.008

Penna, D., van Meerveld, H. J., Oliviero, O., Zuecco, G., Assendelft, R. S., Dalla Fontana, G., & Borga, M. (2015). Seasonal changes in runoff generation in a small forested mountain catchment. *Hydrological Processes*, *29*, 2027–2042. https://doi.org/10.1002/hyp.10347

Philippe, A., & Schaumann, G. E. (2014). Interactions of dissolved organic matter with natural and engineered inorganic colloids: A review. *Environmental Science & Technology*, *48*, 8946–8962.

Ranville, J. F., & Macalady, D. L. (1996). Natural organic matter in catchments. In O. M. Seather & P. de Cartitat (Eds.), *Geochemical processes, weathering and groundwater recharge in catchments* (1st ed., pp. 263–304). A. A. Balkema.

Raymond, P. A., & Saiers, J. E. (2010). Event controlled DOC export from forested watersheds. *Biogeochemistry*, *100*, 197–209. https://doi.org/10.1007/s10533-010-9416-7

Reddy, K. R., Diaz, O. A., Scinto, L. J., & Agami, M. (1995). Phosphorus dynamics in selected wetlands and streams of the Lake Okeechobee basin. *Ecological Engineering*, *5*, 183–207. https://doi.org/10.1016/0925-8574(95)00024-0

Regelink, I. C., Koopmans, G. F., van der Salm, C., Weng, L., & van Riemsdijk, W. H. (2013). Characterization of colloidal phosphorus species in drainage waters from a clay soil using asymmetric flow field-flow fractionation. *Journal of Environmental Quality*, *42*, 464–473. https://doi.org/10.2134/jeq2012.0322

Rose, L. A., Karwan, D. L., & Godsey, S. E. (2018). Concentration–discharge relationships describe solute and sediment mobilization, reaction, and transport at event and longer timescales. *Hydrological Processes*, *32*, 2829–2844. https://doi.org/10.1002/hyp.13235

Rosenbaum, U., Bogena, H. R., Herbst, M., Huisman, J. A., Peterson, T. J., Weuthen, A., Western, A. W., & Vereecken, H. (2012). Seasonal and event dynamics of spatial soil moisture patterns at the small catchment scale. *Water Resources Research*, *48*(10).

Rostad, C. E., Leenheer, J. A., & Daniel, S. R. (1997). Organic carbon and nitrogen content associated with colloids and suspended particulates from the Mississippi River and some of its tributaries. *Environmental Science & Technology*, *31*, 3218–3225.

Scherer, W. H. (2009). Sulfur in soils. *Journal of Plant Nutrition and Soil Science*, *172*, 326–335. https://doi.org/10.1002/jpln.200900037

Sebestyen, S. D., Boyer, E. W., & Shanley, J. B. (2009). Responses of stream nitrate and DOC loadings to hydrological forcing and climate change in an upland forest of the northeastern United States. *Journal of Geophysical Research: Biogeosciences*, *114*(G2).

Sebestyen, S. D., Boyer, E. W., Shanley, J. B., Kendall, C., Doctor, D. H., Aiken, G. R., & Ohte, N. (2008). Sources, transformations, and hydrological processes that control stream nitrate and dissolved organic matter concentrations during snowmelt in an upland forest. *Water Resources Research*, *44*(12).

Sharma, R., Bell, R. W., & Wong, M. T. F. (2017). Dissolved reactive phosphorus played a limited role in phosphorus transport via runoff, throughflow and leaching on contrasting cropping soils from southwest Australia. *Science of the Total Environment*, *577*, 33–44. https://doi.org/10.1016/j.scitotenv.2016.09.182

Sharpley, A. N., Jarvie, H. P., Buda, A., May, L., Spears, B., & Kleinman, P. J. (2013). Phosphorus legacy: Overcoming the effects of past management practices to mitigate future water quality impairment.

Journal of Environmental Quality, *42*, 1308–326. https://doi.org/10.2134/jeq2013.03.0098

Six, J., Elliot, E. T., & Paustian, K. (1999). Aggregate and soil organic matter dynamics under conventional and no-tillage systems. *Soil Science Society of America Journal*, *63*, 1350–1358. https://doi.org/10.2136/sssaj1999.6351350x

Stacy, E. M., Hart, S. C., Hunsaker, C. T., Johnson, D. W., & Berhe, A. A. (2015). Soil carbon and nitrogen erosion in forested catchments: Implications for erosion-induced terrestrial carbon sequestration. *Biogeosciences*, *12*, 4861–4876. https://doi.org/10.5194/bg-12-4861-2015

Stockinger, M., Bogena, H. R., Lücke, A., Diekkrüger, B., Weiler, M., & Vereecken, H. (2014). Seasonal soil moisture patterns: Controlling transit time distributions in a forested headwater catchment. *Water Resources Research*, *50*, 5270–5289. https://doi.org/10.1002/2013WR014815

Stolpe, B., Guo, L., Shiller, A. M., & Aiken, G. R. (2013). Abundance, size distributions and trace-element binding of organic and iron-rich nanocolloids in Alaskan rivers, as revealed by field-flow fractionation and ICP-MS. *Geochimica Et Cosmochimica Acta*, *105*, 221–239. https://doi.org/10.1016/j.gca.2012.11.018

Strohmeier, S., Knorr, K. H., Reichert, M., Frei, S., Fleckenstein, J. H., Peiffer, S., & Matzner, E. (2013). Concentrations and fluxes of dissolved organic carbon in runoff from a forested catchment: Insights from high frequency measurements. *Biogeosciences*, *10*, 905–916. https://doi.org/10.5194/bg-10-905-2013

Stutter, M. I., Langan, S. J., & Cooper, R. J. (2008). Spatial contributions of diffuse inputs and within-channel processes to the form of stream water phosphorus over storm events. *Journal of Hydrology*, *350*, 203–214. https://doi.org/10.1016/j.jhydrol.2007.10.045

Trostle, K. D., Runyon, J. R., Pohlmann, M. A., Redfield, S. E., Pelletier, J., McIntosh, J., & Chorover, J. (2016). Colloids and organic matter complexation control trace metal concentration-discharge relationships in Marshall Gulch stream waters. *Water Resources Research*, *52*, 7931–7944. https://doi.org/10.1002/2016WR019072

Tunaley, C., Tetzlaff, D., Lessels, J., & Soulsby, C. (2016). Linking high-frequency DOC dynamics to the age of connected water sources. *Water Resources Research*, *52*, 5232–5247. https://doi.org/10.1002/2015WR018419

Weigand, S., Bol, R., Reichert, B., Graf, A., Wiekenkamp, I., Stockinger, M., Lücke, A., Tappe, W., Bogena, H., Pütz, T., Amelung, W., & Vereecken, H. (2017). Spatiotemporal analysis of dissolved organic carbon and nitrate in waters of a forested catchment using wavelet analysis. *Vadose Zone Journal*, *16*(3). https://doi.org/10.2136/vzj2016.09.0077

Wiekenkamp, I., Huisman, J. A., Bogena, H., Graf, A., Lin, H. S., Drüe, C., & Vereecken, H. (2016). Changes in measured spatiotemporal patterns of hydrological response after partial deforestation in a headwater catchment. *Journal of Hydrology*, *542*, 648–661. https://doi.org/10.1016/j.jhydrol.2016.09.037

Yusop, Z., Douglas, I., & Nik, A. R. (2006). Export of dissolved and undissolved nutrients from forested catchments in Peninsular Malaysia. *Forest Ecology and Management*, *224*, 26–44. https://doi.org/10.1016/j.foreco.2005.12.006

Zacharias, S., Bogena, H., Samaniego, L., Mauder, M., Fuß, R., Pütz, T., Frenzel, M., Schwank, M., Baessler, C., Butterbach-Bahl, K., Bens, O., Borg, E., Brauer, A., Dietrich, P., Hajnsek, I., Helle, G., Kiese, R., Kunstmann, H., Klotz, S., … Vereecken, H. (2011). A network of terrestrial environmental observatories in Germany. *Vadose Zone Journal*, *10*, 955–973. https://doi.org/10.2136/vzj2010.0139

SUPPORTING INFORMATION

Additional supporting information may be found online in the Supporting Information section at the end of the article.

How to cite this article: Burger DJ, Vogel J, Kooijman AM, Bol R, de Rijke E, Schoorl J, Lücke A, & Gottselig N. Colloidal catchment response to snowmelt and precipitation events differs in a forested headwater catchment. *Vadose Zone J.* 2021*20:*; e20126. https://doi.org/10.1002/vzj2.20126